Journal of Nuclear Medicine & Radiation Therapy

Pereira and Manaças, J Nucl Med Radiat Ther 2019, 10:1
DOI: 10.4172/2155-9619.1000396

Case Series Open Access

Magnetic Resonance Imaging Fusion of Cranial Nerves Impaired by Skull Base Tumors: A Technical Development

Pedro Gonçalves Pereira[1, 2, 3*] **and Rui Manaças**[1]

[1]*Department of Neuroradiology, Hospital Professor Doutor Fernando Fonseca, IC 19 2720-276 Amadora, Portugal*

[2]*Department of Biomedical Sciences and Medicine, University of Algarve, Portugal*

[3]*Algarve Biomedical Center, Gambelas Campus, University of Algarve, Faro, Portugal*

[*]**Corresponding author:** Pedro Goncalves Pereira, Department of Neuroradiology, UALG, Algarve Biomedical Center (ABC), University of Algarve, Portugal, Tel: +351934337817; E-mail: pmgp@mail.com

Received date: February 13, 2019; **Accepted date:** February 28, 2019; **Published date:** March 07, 2019

Abstract

Objectives: Magnetic Resonance Image Fusion is used to highlight tissue characteristics unrevealed by the individual sequences. We have applied a fusion algorithm merging isotropic sequences T2 Constructive Interference in a Steady State-CISS and contrast-enhanced (CE) T1 to obtain multiplanar (MPR) composed images (CESS) of skull base tumors and the surrounding cranial nerves (CN). We hypothesize that CESS images may complement standard Diffusion-Tensor Tractography and depict the deviated trajectories of CN impaired by space occupying lesions within the subaracnoid cisterns.

We describe the fundamentals of this technique and present the cases of several patients in which the information garnered was coincident with CN tractographies and neurosurgical results.

Methods: A retrospective and observational study of six patients (three vestibular schwannomas, two petro-clival meningiomas and one difuse epidermoid) was performed, comparing CESS with CN tractographies and intraoperative findings. Isotropic T2-CISS, pos-Gadolinium T1 images and Diffusion-Tensor (DT) tractographies were obtained preoperatively. MPR fused CESS was processed with the MR vendor's proprietary software.

Results: All fused imaging sets resulted correctly aligned. The location of the CN on CESS was seen has a fiber of low contrast and increased thickness at the tumor margin, coincident with CN tractographies and surgical results.

Conclusion: We speculate that image fusion (CESS) complements CN tractography evaluation and aid in the operative planning.

Keywords: Vestibular schwannoma; Meningioma; Tractography; Diffusion tensor imaging; Fusion imaging; Diagnosis; Computer-assisted

Abbreviations: CN: Cranial Nerve; DT: Diffusion Tensor; CISS: Constructive Interference in a Steady State; CSF: Cerebrospinal Fluid; CE: Contrast-Enhanced; CESS: Image Fusion of 3D T2-CISS and CE 3D-T1; VS: Vestibular Schwannomas

Highlights

- MRI Fusion Techniques may identify Cranial Nerves compressed by Skull-Base Tumors.
- Fused CESS is obtained from standard T2-CISS and pos-Gadolinium T1 sequences.
- CESS compares well with Cranial Nerves (CN) Diffusion-Tensor Tractographies.
- In six patients studied CESS located CN displaced by the tumors.
- CESS is cost-effective means to depict CN impaired by Skull-Base Tumors.

Introduction

Extra-axial masses in the cranial base usually interfere with cranial nerve (CN) function. The goal of surgeries is to remove the largest possible part of the tumor, while preserving CN function. The ability to preserve a compressed CN also depends on the pre-operative identification of the trajectory of the fibber bundles that may be largely deviated from its anatomical location.

With current morphological sequences, the deviated CN trajectories can only be identified if the tumor is small, e.g. vestibular schwannomas of grades 1-2. For larger tumors CN Diffusion-Tensor (DT) tractography is the only means to differentiate soft tissues with similar signal intensities (mass versus CN) [1,2].

However we hypothesised that combining isotropic sequences T2-CISS and T1 with Gadolinium by means of image fusion, we are able to distinguish the CN trajectory at the surface of the tumor.

The Constructive Interference in a Steady State (CISS) sequence is used to delineate milimetric brain structures surrounded by cerebrospinal fluid (CSF). It is particularly useful to identify the cisternal course of CN in the posterior fossa [3].

In T2-CISS water and fat have high signal intensity due to its long T2 and short T1 relaxation times. Additionally there is very low sensitivity to flow and artefacts related with CSF pulsation are minimized. Any soft tissue will appear with equivalent low signal, such has the cranial nerves and space-occupying lesions.

Gadolinium chelates are routinely used in combination with T1-weighted images to enhance lesion morphology and to confirm the neoplastic nature of any intra or extra-axial mass [4]. The gadolinium molecule has a strong paramagnetic effect, induces short T2 and T1 relaxation times and increases the signal intensity in T1 images.

Brain tumor imaging benefits of contrast-enhanced (CE) isotropic T1 acquisitions (higher signal-to- noise ratio, voxel size equal in orthogonal axis), which allows to reformat images in multiple planes with high resolution and to perform volume calculations, two critical items for pre-surgical planning and to assess therapeutical response.

In our institution we use an updated MR protocol to study extra-axial tumors in the skull base, which includes DT tractography, high-resolution T2-CISS and CE 3D-T1 with reasonable acquisition times.

We describe 6 separate neurosurgical cases in which information obtained by image fusion was similar to CN tractographies and confirmed at surgeries.

Materials and Methods

Study population

We have retrospectively studied 6 patients (4 women and 2 men; mean age, 48 years; range, 32-67) with tumors of the posterior fossa (3 vestibular schwannomas, 2 meningiomas and an epidermoid).

Imaging

MR imaging was performed with an Avanto 1.5T scanner (Siemens, Erlanger, Germany) with 8-channel head coil.

The MR protocol was implemented by author P.M.G.P. which includes DT (TR=7100 ms, TE=87 ms, b=1000 s/mm^2, six-axis encoding, FOV=230 mm, matrix=128 × 128, slice thickness=5 mm, slice spacing=3 mm, averaging=4), T2-CISS (TR=5.9 ms, TE=2.7 ms, FOV=200 mm, matrix=512 × 512, slice thickness=0.9 mm) and 3D-T1 gradient-echo (TR 15 ms, TE=4.7 ms, FOV=200 mm, matrix=512 × 512, slice thickness=0.9 mm).

CE 3D-T1 was obtained after a manual intravenous injection of standard dose (0.1 mL/kg) of gadobutrol (Gadovist; Bayer Schering Pharma, Berlin-Wedding, Germany).

Pos-processing (tractography)

DT tractography is performed accordingly to previous described methods [1,2]. Briefly, CN at risk were isolated in the vicinity of each tumor site (facial nerve for patients with cerebellopontine angle VS and trigeminal nerve for meningiomas at pre-pontine cistern and Meckel's cave) using dTV II DT imaging software [5], which performs superselective fiber tractographs using a deterministic algorithm.

Pos-processing (fusion)

Postprocessing of T2-CISS and CE 3D-T1 image fusion (CESS) was implemented with the software Syngo-Fusion provided by the manufacturers of the MR imaging system.

At the workstation the first sequence (T2-CISS) was loaded into MPR within the 3D task-card. Subsequently, we select the CE 3D-T1 data set into the 3D task-card and choose the fusion registration function.

This process automatically aligns and superimpose both data sequences and produces an additional set of 2D multiplanar (MPR; axial, coronal and sagital) fused source images (identified CESS).

To control for any misregistration, we checked whether the boundaries of a normal internal auditory canal where correctly overlaid on MPR CESS as compared with 3D T2-CISS and CE 3D-T1 side by side.

Contrast ratio

Additionally, we calculated the contrast ratio for tissues resulting from image fusion, considering the difference of the signal intensities (SI) divided by the average SI in adjacent regions [6].

We assessed the SI of the CN-location given by tractography versus tumor-core (Contrast 1), and the SI of the tumor-capsule versus tumor-core (Contrast 2) using the equations

Contrast 1 (Eq. A.1):

$$CN/\text{Tumor-core} = (SI_{CN} - SI_{\text{Tumor-core}})/(SI_{CN} + SI_{\text{Tumor-core}})$$

Contrast 2 (Eq. A.2):

$$\text{Tumor-capsule}/\text{Tumor-core} = (SI_{\text{Tumor-capsule}} - SI_{\text{Tumor-core}})/(SI_{\text{Tumor-capsule}} + SI_{\text{Tumor-core}})$$

Where SI corresponds to intensities obtained from manually drawn point-based ROIs with the same number of pixels for each case.

Surgeries

Patients with VS and meningiomas underwent surgeries between October 2011 and September 2015 (Table 1).

Vestibular Schwannomas and petro-clival meningiomas were operated using a retrosigmoid pathway to assess the ipsilateral cerebello-pontine angle.

In the case of VS, the facial nerve position was confirmed using a bipolar electrode that delivered successive electric stimulus of low-intensity (less than 0.5 mA) and short-duration (less than 0.5 ms) in the tumor surface.

The origin of the trigeminal nerve in the Pons was identified in both meningioma cases and followed distally up to Meckel´s cave as the the tumor mass was debulked.

Case Series

Pathologic entities include 3 vestibular schwannomas VS, 2 meningiomas and an epidermoid; classification of VS accordingly to Koos scale [7]. Patients with VS and meningiomas were operated with a favourable postsurgical follow-up, without CN deficits.

There was a complete agreement between the facial and trigeminal course depicted pre-operatively by tractography and the position of these CN during the surgical procedures (Table 1). The retrospective analysis of CESS showed similar results compared to CN tractographs (Table 1).

Patient	Demographics	Diagnosis	Tractography	CESS	Surgical Findings
1	M; 39 y	VS gr.3, L-CPA	Facial Antero-Inferior Shift	Facial Antero-Inferior Shift	Facial Antero-Inferior Shift
2	F; 55 y	VS gr.4, L-CPA	Facial Anterior Shift	Facial Anterior Shift	Facial Anterior Shift
3	M; 42 y	VS gr.4, R-CPA	Facial Anterior Shift	Facial Anterior Shift	Facial Anterior Shift
4	F; 67 y	Mening, R-petroclival	Trigeminal Lateral Shift	Trigeminal Lateral Shift	Trigeminal Lateral Shift
5	F; 61 y	Mening, L-petrous	Trigeminal Medial Shift	Trigeminal Medial Shift	Trigeminal Medial Shift
M: Male; F: Female; VS: Vestibular Schwannoma; Mening: Meningioma; CPA: Cerebellopontine Angle					

Table 1: Patients demographics, diagnosis, tractography of cn, visualization of cn by cess and agreement with surgical findings.

CESS images resulted in fused MPR data sets clearly aligned and with additional contrast information obtained from the tumor and surrounding structures (Table 2). There were no signal artifacts resulting from the image fusion pos-processing.

Patient	Diagnosis	Contrast 1	Contrast 2	% difference
1	VS gr.3, L-CPA	-0,34	-0,17	49
2	VS gr.4, L-CPA	-0,32	-0,12	63
3	VS gr.4, R-CPA	-0,48	-0,10	79
4	Mening, R-petroclival	-0,37	-0,10	73
5	Mening, L-petrous	-0,58	-0,24	59
VS: Vestibular Schwannoma; Mening: Meningioma; Contrast ratio was calculated on fused images using the formula Contrast A/B=(SIA - SIB)/(SIA + SIB), where SIA and SIB correspond to intensities obtained from manually drawn point-based ROIs ; Contrast 1 (contrast difference between the location of the CN and the central enhancing region of the tumor) ; Contrast 2 (contrast difference between the tumor capsule and the central enhancing region of the tumor); % difference between Contrast 1 and 2.				

Table 2: Quantitative analysis of cess. contrast ratio for tissues resulting from image fusion.

Cases 1-3: Vestibular Schwannomas

Case 1 is a 39- years old male with left-side solid grade 3 VS (Figures 1A and 1B). CESS (Figures 1C and 1F) shows a linear and stretched structure at the tumor periphery, similar to the course depicted by tractography (Figures 1D and 1E). Beside bone, the signal is lower than any of the remaining tissues. The facial nerve was seen at an antero-inferior position at surgery (Figure 1).

Case 2 is a 55-year-old female with left- side cystic grade 4 VS (Figures 2A and 2B). The facial nerve was deviated anteriorly has depicted both by tractography (Figure 2C) and surgery, similar to the linear, hypointense and distorted structure at the tumor periphery seen by CESS (Figure 2).

Case 3 is a 42-year-old male with right-side solid VS (Figures 3A and 3B). Tractography (Figure 3C) shows the facial nerve with conventional color-coded directions, at similar position revealed by surgery. CESS (Figure 3D) defines an identical facial nerve tract (Figure 3).

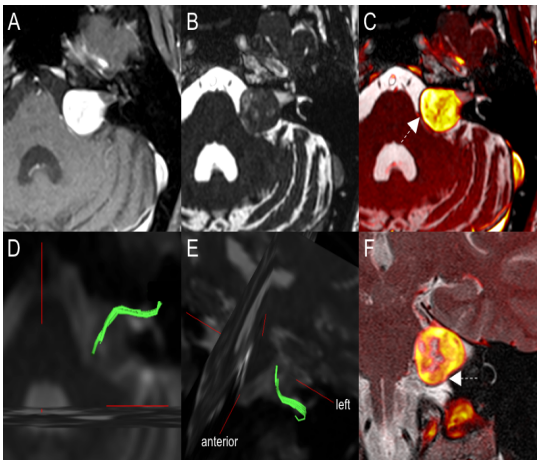

Figure 1: (A) Axial CE 3D-T1, (B) Axial 3D T2-CISS, (C) Axial MPR fused CESS, with arrow pointing the facial nerve, (D) Axial Tractography of the facial nerve without conventional color-coded directions, (E) Superior and left view of Tractography of the facial nerve, (F) Coronal MPR CESS, with arrow pointing the facial nerve.

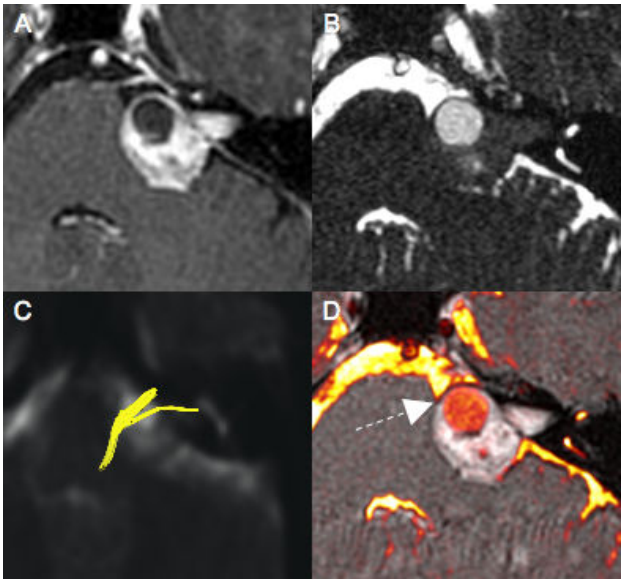

Figure 2: (A) Axial CE 3D-T1, (B) Axial 3D T2-CISS, (C) Axial Tractography of the facial nerve, (D) Axial MPR CESS, with arrow pointing the facial nerve.

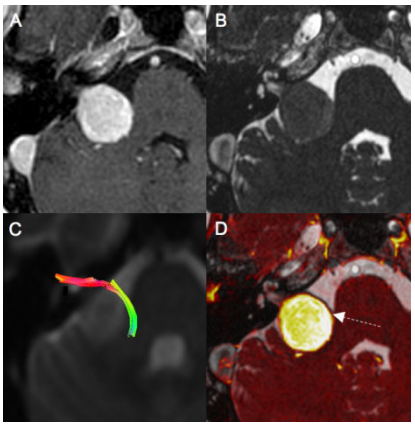

Figure 3: (A) Axial CE 3D-T1, (B) Axial 3D T2-CISS, (C) Axial tractography of the facial nerve, (D) Axial MPR CESS, with arrow pointing the facial nerve.

Cases 4 and 5: Meningiomas

Case 4 is a 67-year-old female with right-side petro-clival meningioma impinging on the ipsilateral trigeminal nerve. CESS (Figures 4A-4C) and tractography (Figures 4D-4F) show that the trigeminal nerve is laterally deviated from its normal position (Figure 4).

Case 5 is a 61-year-old female with left-side petrous meningioma invading the ipsilateral Meckel cave. The trigeminal nerve is indistinguishable from the tumor mass in CE 3D-T1 (Figure 5A) and 3D T2-CISS (Figure 5B). Applying CESS (Figures 5C and 5D) allows depicting the trigeminal nerve compressed medially accordingly with tractography (not shown) (Figure 5).

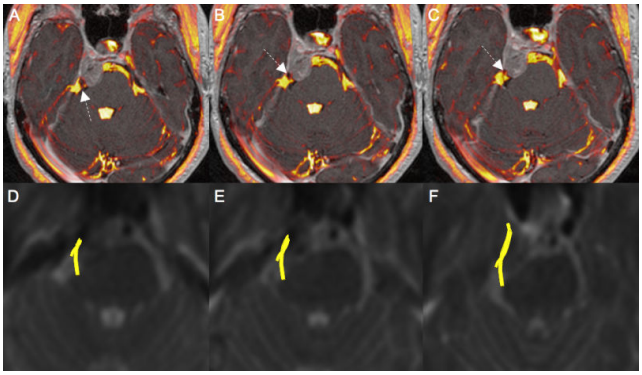

Figure 4: (A-C) Axial MPR CESS, with arrow pointing the right side trigeminal nerve, (D-F) axial tractography of the right side trigeminal nerve.

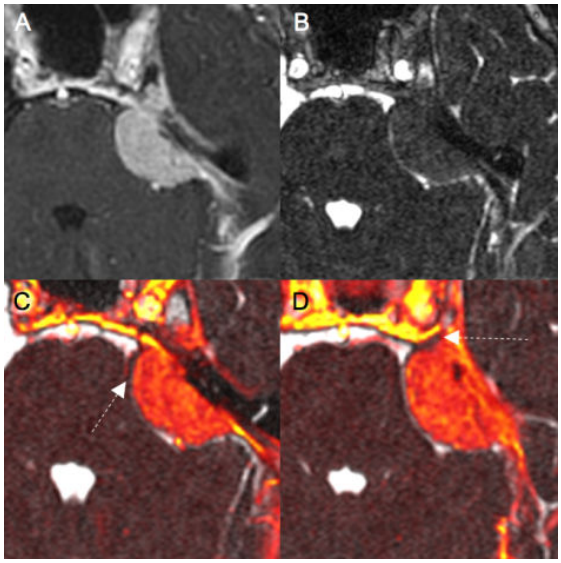

Figure 5: (A) Axial CE 3D-T1, (B) Axial 3D T2-CISS, (C and D) Axial MPR CESS, with arrow pointing the trigeminal nerve.

Case 6: Epidermoid of the Basal Cisterns

Case 6 is a 36-year-old female with a difuse epidermoid filling the basal cisterns, engulfing several CN, veins and arteries. Although the relationship between the lobulated macrostructure of the tumor and CN is depicted by 3D T2-CISS, a clear distinction between CN, vascular elements and mass is best archived with CESS. Additionally most of the CN can be depicted sequentially with CESS, while current CN tractography is performed for each CN making this a laborious and time. Consuming technique when large or infiltrating tumors compromise several nerve fibers (Figure 6).

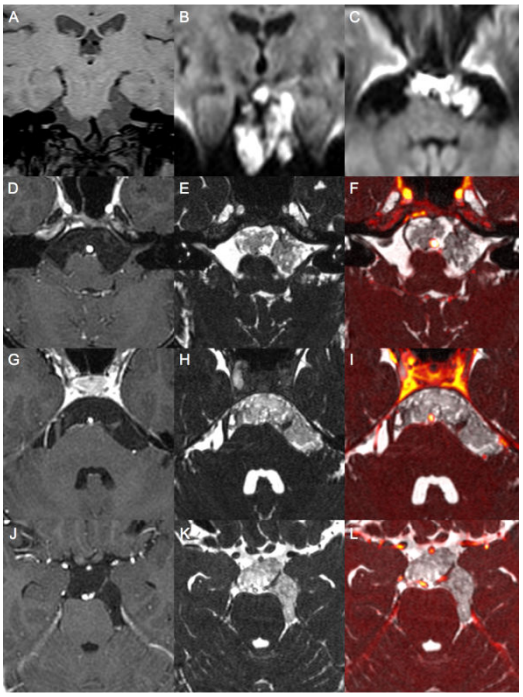

Figure 6: (A) Coronal non-enhanced T1-fatsat, (B) Coronal DWI, (C) Axial DWI, (D, G and J) Axial CE 3D-T1, (E, H and K) Axial 3D T2-CISS, (F, I and L) Axial MPR CESS.

Discussion

In this preliminary case series, we have seen the possibility to identify displaced CN due to its intrinsic contrast properties by fusing standard MR sequences 3D T2-CISS and CE 3D-T1.

Moreover, CESS imaging showed equivalent results when compared to tractography of the Facial and Trigeminal nerves that were separately compressed by schwannomas and meningiomas and engulfed by an epidermoid cyst in these different patients.

The common characteristics highlighted by CESS imaging were (1) the hiposignal of the compressed CN compared with the high signal of the tumor and the highest signal of CSF, (2) a difference in thickness across tumor surfaces, which was larger on the side of the distorted CN and (3) in plane contrast gradient across tissues (high CSF/low CN/high tumor-core/intermediate tumor-capsule/high CSF).

A possible explanation for this change in signal and increased thickness that allows visualization of the CN is tissue oedema and inflammation of the nerve fibers compressed by tumor mass. These reactive phenomena allow displaying different tissue characteristics when compared to normal CN that were only highlighted by fusing imaging modalities.

CESS may also prove a complementary diagnostic tool regarding tractographies of CN. Fusion software is simpler to use than DT tractography. The results of the CESS technique can be obtained rapidly and provide preliminary information regarding the displacement of the CN. Eventually it can also be used to facilitate the tractography post-processing by pointing the probable location of the CN at risk.

Acknowledgment

To the neurosurgical team that operated these different patients. Victor Gonçalves with Anabela Nabais, Luis Mateus and Victor de Sousa for providing the surgical location of the CN affected by the tumors.

To Municipality of Loulé, Portugal.

References

1. Taoka T, Hirabayashi H, Nakagawa H, Sakomoto M, Myochin K, et al. (2006) Displacement of the facial nerve course by vestibular schwannoma: Preoperative visualization using diffusion tensor tractography. J Magn Reson Imaging 24: 1005-1010.
2. Goncalves - Pereira PM, Manaças R, Neto d´Almeida G, Escada P, Goncalves V, et al. (2015) Pre-operative cranial nerve tractography in skull base otoneurosurgeries: Results of 76 Cases. Neuroradiology 57: 418.
3. Casselman JW, Kuhweide R, Deimling M, Ampe W, Dehaene I, et al. (1993) Constructive interference in steady state-3dft MR imaging of the cerebellopontine angle. AJNR Am J Neuroradiol 14: 47-57.
4. Kanal E, Maravilla K, Rowley HA (2014) Gadolinium contrast agents for cns imaging: Current concepts and clinical evidence. AJNR Am J Neuroradiol 35: 2215-2226.
5. Masutani Y, Aoki S, Abe O, Hayashi N, Otomo K (2003) MR diffusion tensor imaging: Recent advance and new techniques for diffusion tensor visualization. Eur J Radiol 46: 53–66.
6. Brix G, Kolem H, Nitz WR (2008) Image contrast and imaging sequences. In: Reiser FM, Semmler W, Hricak H (eds). Magnetic resonance tomography. Springer-Verlag, Berlin Heidelberg, pp 36-75.
7. Koos WT, Day JD, Matula C, Levy DI (1998) Neurotopographic considerations in the microsurgical treatment of small acoustic neurinomas. J Neurosurgery 88: 506-512.